

Lateralization, maturation, and anteroposterior topography in the lateral habenula revealed by ZIF268/EGR1 immunoreactivity and labeling history of neuronal activity

Abbreviated title: Habenular lateralization

Hiroyuki Ichijo^{1,2}, Michito Hamada², Satoru Takahashi^{2,3}, Makoto Kobayashi⁴, Takeharu Nagai⁵, Tomoko Toyama², Masahumi Kawaguchi¹

¹Department of Anatomy, Graduate School of Medicine and Pharmaceutical Sciences, University of Toyama, Toyama 930-0194, Japan

²Department of Anatomy and Embryology, ³Laboratory Animal Resource Center,

⁴Department of Molecular and Developmental Biology, Division of Biomedical Science, Faculty of Medicine, University of Tsukuba, Tsukuba 305-8575, Japan

⁵The Institute of Scientific and Industrial Research, Osaka University, Ibaraki 567-0047, Japan

Corresponding author: Hiroyuki Ichijo

Department of Anatomy, Graduate School of Medicine and Pharmaceutical Sciences, University of Toyama, Sugitani 2630, Toyama 930-0194, Japan

E-mail: ichijo@med.u-toyama.ac.jp

Telephone: +81-76-434-7205

Fax: +81-76-434-5010

Number of pages: 31

Number of figures: 6

Number of Supplementary figures: 7

Number of words for Abstract (163), Introduction (638), and Discussion (2110)

The authors declare no conflict of interest.

Abstract

We report habenular lateralization in a simple transgenic mouse model used for labeling a facet of neuronal activity history. A transgenic construct comprised of a *zif268/egr1* immediate-early gene promoter and a gene for normal Venus fluorescent protein with a membrane tag converted promoter activity into long-life fluorescent proteins, which was thought to describe a facet of neuronal activity history by summing neuronal activity. In addition to mapping the immediate-early gene-immunopositive cells, this method helped demonstrate the functionality of the lateral habenular nucleus (LHb). During postnatal development, the LHb was activated between postnatal days 10 and 16. The water-immersion restraint stress also activated the LHb over a similar period. LHb activation was functionally lateralized, but had no directional bias at the population level. Moreover, the posterior LHb was activated in the early stage after the stress, while the anterior LHb was activated in the later stage. Our results indicate lateralization, maturation, and anteroposterior topography of the LHb during postnatal development and the stress response.

Key words: habenula, fasciculus retroflexus, asymmetry, immediate-early gene, stress.

Introduction

Identifying the neuronal circuits responsible for specific functions is important for understanding the neural basis of animal behaviors. The habenula (Hb) consists of medial and lateral nuclei (MHb and LHb), receives inputs from the basal ganglia and limbic system, extends axons to the fasciculus retroflexus (FR), and sends outputs to forebrain and midbrain nuclei including monoaminergic neurons. The Hb is involved in the regulation of emotional behaviors. In zebrafishes, silencing the MHb activity results in freezing, suggesting its involvement in expression of fear responses ranging from the active coping response of flighting to the passive coping response of freezing (Agetsuma et al., 2010; Okamoto et al., 2012). Another hypothesis suggests that the MHb is involved in controlling levels of anxiety. Because silencing the MHb activity causes elevated levels of anxiety, it may induce greater fear responses, resulting in the transition from active to passive coping (Lee et al., 2010; Mathuru and Jesuthasan, 2013). Further research in mice shows that two parallel pathways through the ventral and dorsal MHb are involved in anxiety- and fear-related behaviors, respectively (Yamaguchi et al., 2013). Neurons in the Hb also respond to stress and aversive stimuli. For instance, neuronal activity as assessed by immediate-early gene (IEG) expression is elevated in the LHb after stress (Wirtshafter et al., 1994; Shumake et al., 2003). Dysfunction of the LHb has been implicated in depression, schizophrenia, and drug addiction (Hikosaka, 2010). Fiber connection from the MHb to the LHb (Kim and Chang, 2005) suggests that the habenular complex integrates information about potentially harmful environments against survival and regulates emotional behaviors. In addition, the Hb shows structural asymmetry in lower vertebrates, thus attracting considerable interest as a model of brain lateralization (Concha et al., 2012). In zebrafish, asymmetry in the dorsal Hb (the fish homolog of the mammalian MHb) is well documented in terms of its development, gross

wiring, and single axon morphology (Aizawa et al., 2005; Gamse et al., 2005; Aizawa et al., 2007; Bianco et al., 2008). It is still unclear whether there is asymmetry in the ventral Hb (the fish homolog of the mammalian LHb) (Amo et al., 2010). Hb asymmetry in mammals is controversial; further investigation is required to understand the links between the structural symmetry and functional lateralization of the Hb (Bianco and Wilson, 2009).

Various methods have been employed for evaluating circuit functionality. IEG expression level is a reliable marker of increased neuronal activity (Saffen et al., 1988; Worley et al., 1993; Zangenehpour and Chaudhuri, 2002; Guzowski et al., 2005); thus, transgenic reporters of neuronal activity that utilize destabilized fluorescent proteins under the control of IEG promoters are useful (Wilson et al., 2002; Barth et al., 2004; Wang et al., 2006; Man et al., 2007; Eguchi and Yamaguchi, 2009; Kawashima et al., 2013). However, fluorescent proteins persist significantly longer than neuronal activity even if they are destabilized. The long-term functions of neuronal circuits can therefore be examined using the slow kinetics of normal fluorescent proteins. Theoretically, neuronal activity history can be described by summing neuronal activity; however, this has not been thoroughly investigated. It is hypothesized that normal long-life fluorescent proteins controlled by IEG promoters are accurate for summing neuronal activity, with the resulting signal indicating a facet of neuronal activity history (Supplementary Fig. 1a–h). To test our hypothesis, we generated transgenic mice having the *zif268/egr1* IEG promoter linked to the normal yellow fluorescent protein gene (*Venus*) with a membrane tag (Man et al., 2007; Arni et al., 1998; Nagai et al., 2002; Slade et al., 2002; Knapska et al., 2004; Barth, 2007). This method was useful in connecting experiences to their corresponding neuronal circuits. By examining a facet of neuronal activity history in addition to mapping the IEG-immunopositive cells, we report the functional lateralization, maturation, and anteroposterior topography of the LHb during postnatal development and water-immersion restraint stress response in mice.

Materials and Methods

Animal experiments were carried out in accordance with the National Institute of Health Guide for the care and use of laboratory animals. All experimental protocols were approved by the Committees for Animal Care and Use of the University of Tsukuba and the University of Toyama. All efforts were made to minimize the number of animals used and their suffering.

Transgenic mice

The gene construct consisted of five elements: a promoter derived from *zif268/egr1*, the QBI SP163 translational enhancer element, a membrane localization sequence, a gene for the brighter variant of the yellow fluorescent protein with normal long-life (*Venus*), and an SV40 poly(A) sequence. The human *egr1* (also called *krox-24*, *zif268*, *TIS8*, or *NGFI-A*) gene was purchased from American Type Culture Collection (ATCC, Manassas, VA; TIS8H7, No. 65849) (Sakamoto et al., 1991). TIS8H7 was amplified using *Pfu* DNA polymerase (Promega, Madison, WI) with the following primers to obtain the *zif268/egr1* promoter (1004-bp length of the 5'-untranslated region of the gene): 5'-end with an *AseI* site, GGGATTAATAATCAGCTTCCCCACTTCGG, and 3'-end with an *XhoI* site, GGGCTCGAGAGTTCTGCGGCTGGATCTCT (Hokkaido System Sciences, Sapporo, Japan). The QBI SP163 element derived from *pcDNA4/HisMaxB* (Invitrogen, Carlsbad, CA) was inserted between the promoter and *Venus*, which functions as a strong translational enhancer through ribosome recruitment and a cap-independent translation mechanism (Stein et al., 1998). The sequence of the 20-amino acids N-terminal fragment of GAP43 was used for membrane localization, which was fused in frame to *Venus* (Supplementary Fig. 1i).

To generate the transgenic mice, the linearized construct (2274 bp) was excised

from the vector, electrophoresed on a 2% agarose gels, purified from the gel, and diluted in 50 ng/ μ L with 100 mM Tris-HCl and 10 mM EDTA (pH 7.4). DNA solution was injected into fertilized oocytes derived from BDF1 mice (Laboratory Animal Resource Center, University of Tsukuba, Tsukuba, Japan). Tail genomic DNA was prepared and germ-line transmission of the transgenes in each line was verified using polymerase chain reaction; the primers were directed against regions in *Venus* (CTGGTCGAGCTGGACGGCGACG and CACGAACTCCAGCAGGACCATG). Nine founder lines were obtained. Five of the nine showed no fluorescence for Venus, and one line exhibited uniform fluorescence for Venus in the brain; the other six lines were not used for further investigations. Three transgenic lines were maintained as heterozygotes and crossed for multiple generations into C57BL/6J mice. To ascertain transgenic integration into the genome, Southern blotting was performed with the probe against *Venus* on the three lines with three restriction enzymes. One of the three lines exhibited a single integration site and this line (*zsgv-a*) was used for experiments in this report. The other two lines were designated as *zsgv-b* and *zsgv-c*. Animals were maintained in single-sex cages with up to five littermates per cage.

Immunohistochemistry and in situ hybridization

Mice were deeply anesthetized with pentobarbital (50 μ g/g body weight) (Dai-nippon Sumitomo Pharma., Osaka, Japan), and transcardially perfused with PBS and 3.7% formaldehyde in PBS. Their brains were immersed in the same fixative at 4°C overnight, embedded in gelatin (16.7% gelatin, 16.7% glycerol in PBS), and post-fixed in the same fixative for 4 d at 4°C. The gelatin block was cut into 70- μ m-thick sections using the Vibratome (VT1500, St. Louis, MO) and rinsed with PBS. Sections were divided into two sets containing every other section. One set was washed in PBS with 0.5% Triton-X100 (PBT), blocked with PBT with 10% normal goat serum, and subsequently stained with a

200-fold dilution of anti-ZIF268/EGR1 antibody (C-19, Santa Cruz Biotechnology, Santa Cruz, CA) with an appropriate secondary antibody coupled with Alexa594 (Invitrogen). The other set was washed in PBS with 0.5% Triton-X100 (PBT) and stained with a 50-fold dilution of NeuroTrace 530/615 red fluorescent Nissl stain (Invitrogen) in PBS for 20 min. The sections were mounted on glass slides in Mowiol 4-88 (Merck Millipore) and observed under a fluorescence microscope (DMRXAA2, Leica, Wetzlar, Germany).

IEG-immunopositive cells in the LHb and labeling in the FR were examined during postnatal development from P9 to P70. The images were obtained with a digital camera (VB-7000, Keyence, Osaka, Japan). They were processed with the same parameters in ImageJ software (National Institutes of Health, Bethesda, MD). The number of immunopositive cells was counted in the LHb.

Brains of the *zsgv-a* transgenic mice were dissected on P13. They were divided into the anterior (including the Hb) and posterior regions (including the FR) by using a stainless brain slicer matrix (Neuroscience Inc., Tokyo, Japan). From the anterior parts, fresh-frozen coronal sections 20 μ m in thickness were prepared and processed for *in situ* hybridization. *Venus* (nucleotides 1–720) was used as template. Digoxigenin-11-UTP (Roche)-labeled cRNA probe was synthesized according to the manufacture instructions. *In situ* hybridization was carried out as described by Esumi et al. (2005). The posterior parts were fixed in 3.7% formaldehyde in PBS, embedded in gelatin and cut into 70- μ m-thick sections using the Vibratome. The sections were stained with NeuroTrace 530/615 red fluorescent Nissl stain.

IEG-immunopositive cells in the LHb after water-immersion restraint stress

For water-immersion restraint stress, mice were placed in a plastic tube and immersed vertically to the level of the xiphoid process in a water bath at 21°C for 1 h on P10, P35, and P60–70 (Miyata et al., 2011). They were perfusion-fixed immediately, 1, 3, 6, 12, or

24 h after either the stress or no stress (control). Their brains were processed for immunohistochemistry against anti-ZIF268/EGR1 and anti-c-Fos antibodies (Ab-2, Merck Millipore, Darmstadt, Germany). Images were obtained with a digital camera under a fluorescence microscope and processed with the same parameters in ImageJ. The number of immunopositive cells was counted in the LHb. Cells were also counted in the thalamic paraventricular nucleus (PV) and the dentate gyrus (DG) as positive and negative controls, respectively, for the stress response. In the LHb and PV, cells were counted from the anterior to posterior. In the DG, they were counted in $250 \times 250\text{-}\mu\text{m}$ area in two sections.

Statistical analyses

Neuronal activity was analyzed in the LHb using a combination of three parameters: $R + L$, $|R - L|$, and $R - L$. The applicability of these parameters for lateralization is theoretically elucidated (Palmer, 1994). “ $R + L$ ” is the number of IEG-immunopositive cells in both sides of the LHb, representing the degree of activation. “ $|R - L|$ ” is the absolute value of the difference of the number of IEG-immunopositive cells between the right and left LHb, representing whether the activation is asymmetrical or not. Moreover, “ $R - L$ ” is the difference in the number of IEG-immunopositive cells between the right and left LHb, representing which side is activated. The averages of $R + L$ were compared between P7–9, P10–12, P13, P14–16, and P17–21 by Kruskal-Wallis rank sum tests and Bonferroni multiple comparisons tests. The averages of $R - L$ and $|R - L|$ were examined by Wilcoxon signed-rank tests.

To examine the effects of water-immersion restraint stress, the averages of $R + L$ were compared between animals that underwent no stress and 0, 1, 3, 6, and 12 h after the stress by Kruskal-Wallis rank sum tests and Bonferroni multiple comparisons tests. The averages of $R - L$ and the averages of $|R - L|$ were examined by Wilcoxon signed-rank tests.

To examine effects of the stress on the activation of the LHb along the anteroposterior axis, the averages of R + L in the anterior sections were compared between animals that underwent no stress and 0, 1, 3, 6, and 12 h after the stress by Kruskal-Wallis rank sum tests and Bonferroni multiple comparisons tests. The averages of R + L in the posterior sections were compared in the same way. The averages of R – L and the averages of |R – L| in the anterior or posterior sections were examined by Wilcoxon signed-rank tests. Differences in the number of immunopositive cells between the anterior and posterior LHb (A – P) were obtained. The averages of A – P were examined by Wilcoxon signed-rank tests. All statistical analyses were carried out using the "R" software (version 2.15.3, The R Foundation for Statistical Computing).

Results

Lateralized activation of the LHb and unilateral Venus labeling in the FR during postnatal development

To select candidates for transgenic constructs, we first performed *in vitro* model experiments for Venus induction and accumulation, confirming low expression of Venus without the stimulus and sharp induction after the stimulus, accumulation of the labeling in a manner proportional to the repetitive stimuli, and gradual decay of the labeling, which can integrate promoter activity (Supplementary Fig. 1). Second, brain slices of parietal cortex were obtained from the transgenic mice generated. Labeling under the influence of electrical stimulation was examined *in vitro*, confirming that labeling reflected the history of electrical stimulation (Supplementary Figs. 2 and 3). Third, we confirmed that the labeling in parietal barrel cortex *in vivo* reflected the sensory experiences of whiskers and the related neuronal activity in the barrel cortex (Supplementary Fig. 4).

The FR is a fiber bundle comprised of axons mainly from the LHb and MHb. We

found unilateral Venus labeling in the FR during postnatal development. Around P13, the FR was unilaterally labeled (Fig. 1a). In cases with intense labeling, the sheath of the FR, where LHb axons are located (Herkenham and Nauta, 1979), was demarcated (Fig. 1b, c). In a case with the most intense labeling, the trajectory from the LHb to the FR sheath was continuously visualized; it was intensely labeled in the ventral FR, moderately labeled in the dorsal FR, and weakly labeled in a ventromedial part of the LHb (Supplementary Fig. 5). Other than that, the FR was segmentally labeled, and the lengths of the labeled segments varied among animals (Fig. 1d, Supplementary Fig. 5). *Venus* mRNA was unilaterally expressed in the LHb on the same side as the fluorescent Venus FR labeling (Supplementary Fig. 5).

The FR was unilaterally labeled between P11 and P20 (53.6% at P13 and 33.3% at P20) (Fig. 1e). The FR was rarely labeled before P10 (0% at P9 and 5.9% at P10) and was not labeled after P35. The labeling was preferentially in the right side on P11, whereas it was in both sides after P13. Neither side of the FR was equally labeled in any of the mice examined. In all mice with FR labeling, labeling in the left and right sides was 45.8% and 54.2%, respectively, showing no directional bias at the population level ($n = 72$) (Fig. 1f). The laterality of labeling was similar between males and females, showing no sexual dimorphism (male left, 45.9%, right, 54.1%, $n = 37$; female left, 45.7%, right, 54.3%, $n = 35$) (Fig. 1g). Unilateral FR labeling was observed in the three independently generated transgenic lines; thus, it was unlikely that the labeling was artificial (Supplementary Fig. 6). Other than the FR, we did not observe unilateral labeling reproducibly in the brains, which supports the idea that neither side was constitutively labeled.

To examine neuronal activity and its correlation with labeling, ZIF268/EGR1-immunopositive cells were examined in the LHb. The immunopositive cells were evenly distributed in the anterior LHb; in contrast, the immunopositive cells formed clusters in the posterior LHb, and some were distributed outside the cluster (Fig. 2). These

patterns of distribution reflected a subnuclear organization of the LHb, indicating functional topography inside the LHb (Andres et al., 1999). The total number of immunopositive cells in both sides of the LHb, R + L, was counted during postnatal development. The averages of R + L were significantly different between the postnatal days (Kruskal-Wallis rank sum test, $\chi^2 = 17.0783$, $p = 0.001866$) (Fig. 3a). There were few immunopositive cells between P7 and P9. A significant number of immunopositive cells was observed between P10 and P16 (P10–P12 versus P7–P9, $p = 0.00183$; P13 versus P7–P9, $p = 0.00064$; P14–P16 versus P7–P9, $p = 0.00074$, Bonferroni multiple comparisons test). The positive cells then decreased in number between P17 and P21. These results show that the LHb was transiently activated between P10 and P16. The increased number of immunopositive cells was correlated with FR labeling (Fig. 1e). To examine neuronal activity between the right and left LHb, we assessed differences in the number of immunopositive cells in the right and left sides, R – L, and the absolute values of the differences, |R – L|. Although the averages of R – L were not significantly different from zero during the postnatal period (Fig. 3b), the averages of |R – L| were significantly different from zero between P10 and P13 (P10–12 and P13, $z = 2.9341$, $p = 0.0009766$, Wilcoxon signed-rank tests) (Fig. 3c). These results show that the LHb was asymmetrically activated between the left and right sides in each animal, but this activation was not biased toward a particular side at the population level.

The number of immunopositive cells in the LHb in each case is shown (Fig. 3d, e). The dominant side of asymmetry varied among the cases. The right side was dominant in cases i–iv, and the left side was dominant in cases v–vi. The results showed individual differences in activation. Moreover, the immunopositive cells were differentially distributed along the anteroposterior axis between the cases. For example, in cases i and ii, more immunopositive cells were found in the anterior than in the posterior LHb. On the other hand, in case v, more immunopositive cells were observed in the posterior LHb than in the anterior

LHb. These results suggest that topographic activation occurs along the anteroposterior axis during postnatal development, in addition to the left-right asymmetry.

Lateralized activation of the LHb and unilateral labeling in the FR induced by water-immersion restraint stress

We examined effects of water-immersion restraint stress on LHb activation patterns (Fig. 4a). For the initial screening, transgenic mice were used. After the stress on P10, unilateral labeling in the FR was observed from 1–3 h and beyond. The unilateral labeling increased to 42.1% (n = 19) 24 h after the stress (Fig. 4b–d). Cases with intense labeling showed labeling in the core and sheath of the FR (Fig. 4b, c). The labeling was preferentially in the right side 6 h after the stress, whereas it was in both sides 24 h after the stress. Neither side of the FR was equally labeled in any of the mice examined. In all mice with FR labeling (n = 8), labeling in the left and right sides was 50.0% and 50.0%, respectively, showing no directional bias at the population level. The stress did not induce labeling on P35 or later (Fig. 4e), indicating that the induction depended on the maturation stage of the mice.

In the LHb, a significant number of ZIF268/EGR1-immunopositive cells, R + L, was observed after the stress (Figs. 5, 6) (1 h after the stress in both sides of the LHb, Kruskal-Wallis rank sum test, $\chi^2 = 16.2277$, $p = 0.006223$; control versus 1 h after the stress, $p = 0.039$, Bonferroni multiple comparisons test) (Fig. 5a). The intense immunopositive cells were observed in the medial portion of the anterior LHb (Fig. 6c) as described by Wirtshafter et al. (1994). The average of R + L was decreased 6 h after the stress. These results show that the LHb was transiently activated. To compare the activation between the right and the left sides, differences in the number of immunopositive cells between the two sides, R – L, and the absolute values of the differences, |R – L|, were examined. Although the averages of R – L were not significantly different from zero before and after the stress (Fig. 5b), the averages

of $|R - L|$ were significantly different from zero from immediately after the stress to 6 h after the stress (0 h, $z = 2.6703$, $p = 0.003906$; 1 h, $z = 2.2014$, $p = 0.03125$; 3 h, $z = 2.6679$, $p = 0.003906$; 6 h, $z = 2.6679$, $p = 0.003906$, Wilcoxon signed-rank tests) (Fig. 5c).

c-Fos-immunopositive cells were also examined in the LHb (Supplementary fig. 7). Many c-Fos-immunopositive cells, $R + L$, were observed 3 and 6 h after the stress although the numbers of positive cells varied among the cases (for example, from 193 to 1116 cells at 3 h after the stress). The wide variances might be due to differences in induction of c-Fos by the stress at P10 since alternate sections from the same cases were used for ZIF268/EGR1 and c-Fos immunohistochemistry. Average differences, $R - L$, were not significantly different from zero, and averages of absolute values of the differences, $|R - L|$, were significantly different from zero from 3 to 6 h after the stress.

As control experiments, effects of the stress were examined in the PV, which is known to respond to conditioned fear (Beck and Fibiger, 1995), and in the DG, which is not known to respond to stress. In the PV, a significant number of ZIF268/EGR1-immunopositive cells, $R + L$, was observed 3 h after the stress in both sides (Kruskal-Wallis rank sum test, $\chi^2 = 16.7073$, $p = 0.00509$; control versus 3 h, $p = 0.0099$, Bonferroni multiple comparisons test) (Fig. 5d). The averages of $R - L$ were significantly different from zero immediately or 3 h after the stress (0 h, $z = -2.4565$, $p = 0.01562$; 3 h, $z = -2.0769$, $p = 0.03516$, Wilcoxon signed-rank tests) (Fig. 5e). The averages of $|R - L|$ were significantly different from zero immediately, 3, and 6 h after the stress (0 h, $z = 2.4565$, $p = 0.01562$; 3 h, $z = 2.6703$, $p = 0.003906$; 6 h, $z = 2.6155$, $p = 0.007812$, Wilcoxon signed-rank tests) (Fig. 5f). These results indicate that the stress asymmetrically activated the PV on a different time scale with a possible directional bias at the population level. In the DG, the averages of $R + L$ and $R - L$ were not significantly different before and after the stress (Fig. 5g, h). The averages of $|R - L|$ were significantly different from zero (0 h, $z = 2.4565$, $p =$

0.01562; 3 h, $z = 2.5298$, $p = 0.007812$; 6 h, $z = 2.5236$, $p = 0.007812$, Wilcoxon signed-rank tests) (Fig. 5i). These results indicate that neuronal activity in the DG did not correlate with the stress, although it was lateralized with no directional bias at the population level.

Topographic activation of the LHb along the anteroposterior axis

To examine the topographic activation of the LHb, the distribution of ZIF268/EGR1-immunopositive cells was examined along the anteroposterior axis after the water-immersion restraint stress. While more immunopositive cells were observed in the posterior LHb 1 h after the stress, they were observed in the anterior LHb 3 h after the stress (Fig. 6a-d). A significant number of immunopositive cells, R + L, was observed in the posterior LHb 1 h after the stress (Kruskal-Wallis rank sum test, $\chi^2 = 12.9025$, $p = 0.02431$; 1 h versus control, $p = 0.016$, Bonferroni multiple comparisons test). In the anterior LHb, a significant number of immunopositive cells, R + L, was observed 3 h after the stress (Kruskal-Wallis rank sum test, $\chi^2 = 14.77$, $p = 0.01139$. 3 h versus control, $p = 0.048$, Bonferroni multiple comparisons test) (Fig. 6e). The averages of R – L were not significantly different from zero before and after the stress in both the anterior and posterior LHb (Fig. 6f). The averages of |R – L| were significantly different from zero after the stress in both the anterior LHb (0 h, $z = 2.6679$, $p = 0.003906$; 1 h, $z = 2.2014$, $p = 0.03125$; 3 h, $z = 2.6679$, $p = 0.003906$; 6 h, $z = 2.6132$, $p = 0.007812$, Wilcoxon signed-rank tests) and posterior LHb (0 h, $z = 2.6656$, $p = 0.003906$; 1 h, $z = 2.2014$, $p = 0.03125$; 3 h, $z = 2.6202$, $p = 0.007812$; 6 h, $z = 2.6679$, $p = 0.003906$, Wilcoxon signed-rank tests) (Fig. 6g). The results show that the stress activated the posterior LHb earlier and anterior LHb later. Moreover, differences in the number of immunopositive cells between the anterior and posterior LHb, A – P, were examined. The average of A – P was significantly larger than zero 3 h after the stress (average = 61.7, $z = 2.3122$, $p = 0.01953$, Wilcoxon signed-rank test), confirming the

topographic activation along the anteroposterior axis.

Discussion

Labeling a facet of neuronal activity history

IEG expression is a reliable marker of increased neuronal activity; therefore, transgenic mice expressing destabilized short-lifetime fluorescent proteins under the control of IEG promoters have been generated as reporters of neuronal activity (Worley et al., 1993; Wilson et al., 2002; Barth et al., 2004; Guzowski et al., 2005; Wang et al., 2006; Man et al., 2007; Eguchi and Yamaguchi, 2009; Kawashima et al., 2013). In transgenic mice with a *fosEGFP* fusion gene, expression of *fosEGFP* was maximal 1–2 h after stimulation and declined to baseline levels by 4–8 h, thus showing a time course similar to that of intrinsic c-Fos expression (Barth et al., 2004). Their method makes activated regions in the brain observable at a cellular resolution without fixation and demonstrated functionality in neuronal circuits *in vivo*, confirming the utility of these approaches and showing how different brain areas function. However, the expression kinetics of the intrinsic IEG products and their reporters with destabilized proteins differ from the kinetics of neuronal activity itself (hours vs. milliseconds, respectively) (Saffen et al., 1988; Zangenehpour and Chaudhuri, 2002). The number of ZIF268/EGR1-immunopositive cells reflects neuronal activity that occurred several hours before fixation because the lifetime of the ZIF268/EGR1 protein is several hours (Miyashita et al., 2009).

We used a simple transgenic reporter with a normal, long-half-life fluorescent protein under the control of the IEG promoter. The reporter accumulated the labeling in a manner proportional to repetitive stimuli and showed gradual decay of the labeling, which can integrate neuronal activity (Supplementary Fig. 1), whereas the IEG proteins showed no accumulation. The *in vitro* labeling gradually decayed in about 5 d although the labeling

intensity was affected by cell proliferation and growth in this model experiments *in vitro*. In the transgenic mice, the *in vivo* labeling intensity was reduced 5 d after whisker removal in the barrel cortex (Supplementary Fig. 4), and the unilateral FR labeling persisted for several days (Fig. 1). Specifying the exact length of the integration window was not easy; however, both the *in vitro* and *in vivo* results suggest that it is on the order of days. Thus, the transgenic mice we used are rather suitable for examining long-term events.

However, this method has its limitations. For example, there is no control when the accumulation of the labeling begins and ends. Therefore, intense labeling made it difficult to discriminate specific signals after P30, which is likely due to natural neuronal activity in daily life (data not shown). This method would be more valuable if the time window of neuronal activity observation could be regulated. In spite of its limitations, labeling a facet of neuronal activity history offered a way to uncover LHb functionality, which we discuss in the next section.

Lateralization of the LHb

The LHb is known to process negative motivational information elicited by aversive stimuli and stress (Wirtshafter et al., 1994; Shumake et al., 2003; Matsumoto and Hikosaka, 2007; Matsumoto and Hikosaka, 2009). We observed unilateral FR labeling in three independently generated transgenic lines, which is thought to be controlled by the *zif268/egr1* promoter and is not caused by artificial expression such as the location of the transgenic insertion site in the genome. The unilateral FR labeling indicated a lateralized increase of neuronal activity in the Hb during postnatal development and after water-immersion restraint stress. To confirm this idea, we counted the number of IEG-immunopositive cells in the LHb. Considerable IEG immunoreactivity was also observed in the MHb after the stress, suggesting that the MHb was also activated by the stress. However, small sizes and greater densities of the cells in the

MHb prevented us from counting the cells (data not shown). Thus, this discussion is confined to the LHb.

The neuronal activity was analyzed in the LHb using a combination of three parameters. " $R + L$ " represents the degree of activation. " $|R - L|$ " represents whether the activation is asymmetrical or not. " $R - L$ " represents which side is activated. The average of $R + L$ was increased 1 h after the stress prior to the FR labeling at 6 h (Fig. 5). The results confirmed that the LHb was transiently activated after the stress as shown by Wirtshafter et al. (1994). During postnatal development after P10, the elevated neuronal activity in the LHb coincided with the onset of visual experiences and functional hearing (Fig. 3) (Shnerson et al., 1981; Sanes and Constantine-Paton, 1985; Hooks and Chen, 2007). Because the onset of sensory experiences allows immature mice to experience their outer world, it might be stressful and aversive for mice to prepare for their survival, which could indirectly explain the elevated LHb neuronal activity during postnatal development.

The average of $|R - L|$ was significantly different from zero during postnatal development and after the stress, which was correlated with LHb activation as shown by the average of $R + L$ (Figs. 3, 5). These results show that LHb activation was asymmetric. However, the average of $R - L$ was not significantly different from zero throughout the analyses, which indicated that the activated sides were random at the population level. Therefore, these results support that the LHb was functionally lateralized with no directional bias at the population level during both postnatal development and the stress response. This agrees with the unilateral labeling in the FR, which showed no directional bias at the population level (Figs. 1, 4). Because the LHb receives unilateral input from the stria medullaris and projects bilaterally to the monoaminergic nuclei (Herkenham and Nauta, 1977; Herkenham and Nauta, 1979), the unilateral LHb activation may result from lateralized input and function in propagating its information bilaterally.

To confirm the effects of water-immersion restraint stress, we counted the number of IEG-immunopositive cells in the PV. The PV should be activated by the stress because it is activated during conditioned fear (Beck and Fibiger, 1995). The average of R + L showed that the PV was activated 3 h after the stress. The averages of |R – L| and R – L were significantly different from zero after the stress (Fig. 5d–f). The results indicated that the stress asymmetrically activated the PV on a different time scale with a possible directional bias at the population level. We also counted the number of IEG-immunopositive cells in the DG, which is not known to respond to stress. The averages of R + L showed that the neuronal activity in the DG was not correlated with the response to the stress. The averages of |R – L| were significantly different from zero, and the averages of R – L were not significantly different from zero (Fig. 5g–i). As expected, the neuronal activity in the DG did not correlate with the stress, although it was lateralized with no directional bias at the population level. These results confirmed the specificity of the stress effects on the LHb and PV, and the value of the parameters for testing the lateralization of neuronal activity.

The results support that the LHb was laterally activated during development from P10 to P16 and after water-immersion restraint stress, which induced the lateralized expression of Venus in the LHb. Expression of *Venus* mRNA in the unilateral LHb was shown in the same side of the Venus FR labeling (Supplementary fig. 5). The results confirmed lateralized increase of the neuronal activity in the LHb but excluded lateralized degradation of Venus. Because of the *GAP-43* membrane localization sequence linked to *Venus*, the labeling was localized to the cell surface (Supplementary Fig. 1). However, other than the case with the most intensely labeled FR, the labeling did not appear in the LHb or in the entire length of the FR, but did appear in segments along the FR (Fig. 1, and Supplementary Fig. 5). In axon tracing with lipophilic tracers, if given enough time, large amounts of the tracers label entire neurons from the soma to axon terminals, but a small

amount labels the membrane vesicles along the axon or part of the axon (Ichijo, 1999; Ichijo and Toyama, 2014). The LHb neurons may produce insufficient Venus to label the entire cell surface, but could produce a small amount of Venus transiently, which would then be transported down the axons and result in the segmental FR labeling. Thus, the labeling of Venus is thought to depend on at least two factors: neuronal activity resulting in amount of Venus expression and accumulation of Venus in neurons. These factors might set a threshold of Venus labeling. Although neuronal activity shown by IEG positive cells was moderately lateralized, Venus labeling in the FR was clearly lateralized; this might be due to the effect of threshold for Venus labeling and its enhancement. About half of the mice showed unilateral labeling in the FR during postnatal development and after the stress. Because neuronal activity in the LHb was lateralized regardless of the labeling, a threshold of neuronal activity might be required for the labeling to occur.

IEG expression and FR labeling were lateralized; however, it was difficult to correlate the laterality of IEG expression with that of FR labeling in the same mice because it is impossible to fix the same mice twice. Thus, our experiments did not reveal whether the same side of the LHb is consistently activated or not. In both development and water-immersion restraint stress response, the right FR is labeled in the early stage (P11 and 6 h after the stress); then, the left FR labeling appears in late stage (P13 and 24 h after the stress)(Figs. 1 and 4). The shift of the labeling between the right and left from the early to late stages is common during development and the stress response. These results indicate that lateralization of the LHb is not restricted to either side; rather, the LHb is dynamically activated between the right and left sides. The LHb lateralization shown in this report could possibly be caused by oscillatory activation between the right and left LHb in development and the stress response. To solve this problem, further electrophysiological study would be informative.

Labeling a facet of neuronal activity history was useful for finding the lateralized activation of the LHb over a short duration because it allowed the transient increase of neuronal activity to be observable for a longer period; thus, it could be easily detected. Moreover, spontaneous activation during postnatal development labeled the sheath of the FR, whereas exposure to water-immersion restraint stress labeled the core and sheath of the FR (Figs. 1, 4). These results indicate that the different experiences labeled distinct circuits because the MHb and LHb axons run in the core and sheath, respectively (Herkenham and Nauta, 1979). They support the idea that labeling a facet of neuronal activity history is useful for relating experiences with their corresponding neuronal circuits. The IEG immunoreactivity suggests that the MHb was also activated after the stress. It will also be important to examine the lateralization of the MHb after the stress because the MHb homologue in zebrafish, the dorsal Hb, has been a main target of investigation for neuronal circuit asymmetry (Aizawa et al., 2005; Gamse et al., 2005; Aizawa et al., 2007; Bianco et al., 2008; Agetsuma et al., 2010).

Maturation and anteroposterior topography of the LHb

During the period between P10 and P16, the number of IEG-immunopositive cells increased in the LHb (Fig. 3). The water-immersion restraint stress also increased the number of IEG-immunopositive cells in the LHb over a similar period (Fig. 5). These results suggest functional maturation of the LHb during postnatal development. LHb sensitivity might be maintained at a high level from P10 to P16, and be subsequently downregulated in the later stages of development. These results suggest that a critical period might exist for the stress response; therefore, it would be intriguing to examine the effects of stresses on LHb structure and function at immature stage.

Moreover, the IEG-immunopositive cells were differentially distributed along the

anteroposterior axis in each case during postnatal development, suggesting functional differences in the anterior and posterior LHb (Fig. 3d, e). This was supported by the pattern of topographic activation after water-immersion restraint stress. The number of IEG-immunopositive cells in the posterior LHb peaked 1 h after the stress compared to 3 h after the stress in the anterior LHb (Fig. 6). These results indicated the anteroposterior topography in the LHb. The IEG-immunopositive cells were distributed according to the subnuclei organized along the anteroposterior axis, indicating functional differences among the subnuclei along the anteroposterior axis (Figs. 2, 6) (Andres et al., 1999; Geisler et al., 2003; Aizawa et al., 2012) . Finally, lateralization, maturation, and anteroposterior topography of the LHb are common during postnatal development and the stress response.

Acknowledgements

We thank Dr. Y. Takeuchi for the discussion and Profs. H. Nishijo, and H. Mori for critically reading the manuscript. H.I. designed the project, constructed the transgenes, performed *in vitro* experiments, experiments on the transgenic mice, and wrote the manuscript. T.T. and M.K. performed the experiments on the transgenic mice. T.N. constructed the transgenes and performed the *in vitro* experiments. M.K. constructed the transgenes. M.H. and S.T. generated the transgenic mice. All authors discussed the results and commented on the manuscript. This work was supported by Grants-in-Aids for the 21st Century COE Program, Scientific Research on Priority Areas (C)-Advanced Brain Science Project (13210021), Scientific Research (S) (21220009), Challenging Exploratory Research (26640009) from the Ministry of Education, Culture, Sports, Science, and Technology, Japan, and Grants-in-Aid from Tamura Science and Technology Foundation.

References

- Agetsuma, M., Aizawa, H., Aoki, T., Nakayama, R., Takahoko, M., Goto, M., Sassa, T., Amo, R., Shiraki, T., Kawakami, K., Hosoya, T., Higashijima, S., Okamoto, H., 2010. The habenula is crucial for experience-dependent modification of fear responses in zebrafish. *Nat. Neurosci.* 13, 1354-1356.
- Aizawa, H., Bianco, I.H., Hamaoka, T., Miyashita, T., Uemura, O., Concha, M.L., Russell, C., Wilson, S.W., Okamoto, H., 2005. Laterotopic representation of left-right information onto the dorso-ventral axis of a zebrafish midbrain target nucleus. *Curr. Biol.* 15, 238-243.
- Aizawa, H., Goto, M., Sato, T., Okamoto, H., 2007. Temporally regulated asymmetric neurogenesis causes left-right difference in the zebrafish habenular structures. *Dev. Cell* 12, 87-98.
- Aizawa, H., Kobayashi, M., Tanaka, S., Fukai, T., Okamoto, H., 2012. Molecular characterization of the subnuclei in rat habenula. *J. Comp. Neurol.* 520, 4051-4066.
- Amo, R., Aizawa, H., Takahoko, M., Kobayashi, M., Takahashi, R., Aoki, T., Okamoto, H., 2010. Identification of the zebrafish ventral habenula as a homolog of the mammalian lateral habenula. *J. Neurosci.* 30, 1566-1574.
- Andres, K.H., von Duering, M., Veh, R.W., 1999. Subnuclear organization of the rat habenular Complexes. *J. Comp. Neurol.* 407, 130-150.
- Arni, S., Keilbaugh, S.A., Ostermeyer, A.G., Brown, D.A., 1998. Association of GAP-43 with detergent-resistant membranes requires two palmitoylated cysteine residues. *J. Biol. Chem.* 273, 28478-28485.
- Barth, A.L., Gerkin, R.C., Dean, K.L., 2004. Alteration of neuronal firing properties after *in vivo* experience in a FosGFP transgenic mouse. *J. Neurosci.* 24, 6466-6475.
- Barth, A.L., 2007. Visualizing circuits and systems using transgenic reporters of neural activity. *Curr. Opin. Neurobiol.* 17, 567-571.

Beck, C.H., Fibiger, H.C., 1995. Conditioned fear-induced changes in behavior and in the expression of the immediate early gene c-fos: with and without diazepam pretreatment. *J. Neurosci.* 15, 709-720.

Bianco, I.H., Carl, M., Russell, C., Clarke, J.D., Wilson, S.W., 2008. Brain asymmetry is encoded at the level of axon terminal morphology. *Neural Dev.* 3, 9.

Bianco, I.H., Wilson, S.W., 2009. The habenular nuclei: a conserved asymmetric relay station in the vertebrate brain. *Philos. Trans. R. Soc. Lond. B Biol. Sci.* 364, 1005-1020.

Concha, M.L., Bianco, I.H., Wilson, S.W., 2012. Encoding asymmetry within neural circuits. *Nat. Rev. Neurosci.* 13, 832-843.

Eguchi, M., Yamaguchi, S., 2009. *In vivo* and *in vitro* visualization of gene expression dynamics over extensive areas of the brain. *Neuroimage* 44, 1274-1283.

Esumi, S., Kakazu, N., Taguchi, Y., Hirayama, T., Sasaki, A., Hirabayashi, T., Koide, T., Kitsukawa, T., Hamada, S., Yagi, T., 2005. Monoallelic yet combinatorial expression of variable exons of the protocadherin-alpha gene cluster in single neurons. *Nat. Genet.* 37, 171-176.

Gamse, J.T., Kuan, Y.S., Macurak, M., Brösamle, C., Thisse, B., Thisse, C., Halpern, M.E., 2005. Directional asymmetry of the zebrafish epithalamus guides dorsoventral innervation of the midbrain target. *Development* 132, 4869-4881.

Geisler, S., Andres, K.H., Veh, R.W., 2003. Morphologic and cytochemical criteria for the identification and delineation of individual subnuclei within the lateral habenular complex of the rat. *J. Comp. Neurol.* 458, 78-97.

Guzowski, J.F., Timlin, J.A., Roysam, B., McNaughton, B.L., Worley, P.F., Barnes, C.A., 2005. Mapping behaviorally relevant neural circuits with immediate-early gene expression. *Curr. Opin. Neurobiol.* 15, 599-606.

Herkenham, M., Nauta, W.J., 1977. Afferent connections of the habenular nuclei in the rat. A horseradish peroxidase study, with a note on the fiber-of-passage problem. *J. Comp. Neurol.* 173, 123-146.

Herkenham, M., Nauta, W.J., 1979. Efferent connections of the habenular nuclei in the rat. *J. Comp. Neurol.* 187, 19-47.

Hikosaka, O., 2010. The habenula: from stress evasion to value-based decision-making. *Nat. Rev. Neurosci.* 11, 503-513.

Hooks, B.M., Chen, C., 2007. Critical periods in the visual system: changing views for a model of experience-dependent plasticity. *Neuron* 56, 312-326.

Ichijo, H., 1999. Differentiation of the chick retinotectal topographic map by remodeling in specificity and refinement in accuracy. *Dev. Brain Res.* 117, 199-211.

Ichijo, H., Toyama, T., 2014. Axons from the medial habenular nucleus are topographically sorted in the fasciculus retroflexus. *Anat. Sci. Int.* DOI 10.1007/s12565-014-0252-z.

Kawashima, T., Kitamura, K., Suzuki, K., Nonaka, M., Kamijo, S., Takemoto-Kimura, S., Kano, M., Okuno, H., Ohki, K., Bito, H., 2013. Functional labeling of neurons and their projections using the synthetic activity-dependent promoter E-SARE. *Nat. Methods* 10, 889-895.

Kim, U., Chang, S.Y., 2005. Dendritic morphology, local circuitry, and intrinsic electrophysiology of neurons in the rat medial and lateral habenular nuclei of the epithalamus. *J. Comp. Neurol.* 483, 236-250.

Knapska, E., Kaczmarek, L., 2004. A gene for neuronal plasticity in the mammalian brain: Zif268/Egr-1/NGFI-A/Krox-24/TIS8/ZENK? *Prog. Neurobiol.* 74, 183-211.

Lee, A., Mathuru, A.S., Teh, C., Kibat, C., Korzh, V., Penney, T.B., Jesuthasan, S., 2010. The habenula prevents helpless behavior in larval zebrafish. *Curr. Biol.* 20, 2211-2216.

Man, P.S., Wells, T., Carter, D.A., 2007. Egr-1-d2EGFP transgenic rats identify transient populations of neurons and glial cells during postnatal brain development. *Gene Expr. Patterns* 7, 872-883.

Mathuru, A.S., Jesuthasan, S., 2013. The medial habenula as a regulator of anxiety in adult zebrafish. *Front. Neural Circuits* 7, 99. doi: 10.3389/fncir.2013.00099.

Matsumoto, M., Hikosaka, O., 2007. Lateral habenula as a source of negative reward signals in dopamine neurons. *Nature* 447, 1111-1115.

Matsumoto, M., Hikosaka, O., 2009. Representation of negative motivational value in the primate lateral habenula. *Nat. Neurosci.* 12, 77-84.

Miyashita, T., Kubik, S., Haghighi, N., Steward, O., Guzowski, J.F., 2009. Rapid activation of plasticity-associated gene transcription in hippocampal neurons provides a mechanism for encoding of one-trial experience. *J. Neurosci.* 29, 898-906.

Miyata, S., Koyama, Y., Takemoto, K., Yoshikawa, K., Ishikawa, T., Taniguchi, M., Inoue, K., Aoki, M., Hori, O., Katayama, T., Tohyama, M., 2011. Plasma corticosterone activates SGK1 and induces morphological changes in oligodendrocytes in corpus callosum. *PLoS One* 6, e19859.

Nagai, T., Ibata, K., Park, E.S., Kubota, M., Mikoshiba, K., Miyawaki, A., 2002. A variant of yellow fluorescent protein with fast and efficient maturation for cell-biological applications. *Nat. Biotechnol.* 20, 87-90.

Okamoto, H., Agetsuma, M., Aizawa, H., 2012. Genetic dissection of the zebrafish habenula, a possible switching board for selection of behavioral strategy to cope with fear and anxiety. *Dev. Neurobiol.* 72, 386-394.

Palmer, A.R., 1994. Fluctuating asymmetry analyses: a primer. In: Markow, T.A. (Ed.), *Developmental instability: Its origins and evolutionary implications*. Wolters Kluwer, Alphen aan den Rijn, pp. 335-364.

Saffen, D.W., Cole, A.J., Worley, P.F., Christy, B.A., Ryder, K., Baraban, J.M., 1988. Convulsant-induced increase in transcription factor messenger RNAs in rat brain. *Proc. Natl. Acad. Sci. U.S.A.* 85, 7795-7799.

Sakamoto, K.M., Bardeleben, C., Yates, K.E., Raines, M.A., Golde, D.W., Gasson, J.C., 1991. 5' upstream sequence and genomic structure of the human primary response gene, EGR-1/TIS8. *Oncogene* 6, 867-871.

Sanes, D.H., Constantine-Paton, M., 1985. The sharpening of frequency tuning curves requires patterned activity during development in the mouse, *Mus musculus*. *J. Neurosci.* 5, 1152-1166.

Shnerson, A., Devigne, C., Pujol, R., 1981. Age-related changes in the C57BL/6J mouse cochlea. II. Ultrastructural findings. *Brain Res.* 254, 77-88.

Shumake, J., Edwards, E., Gonzalez-Lima, F., 2003. Opposite metabolic changes in the habenula and ventral tegmental area of a genetic model of helpless behavior. *Brain Res.* 963, 274-281.

Slade, J.P., Man, P.S., Wells, T., Carter, D.A., 2002. Stimulus-specific induction of an Egr-1 transgene in rat brain. *Neuroreport* 13, 671-674.

Stein, I., Itin, A., Einat, P., Skaliter, R., Grossman, Z., Keshet, E., 1998. Translation of vascular endothelial growth factor mRNA by internal ribosome entry: implications for translation under hypoxia. *Mol. Cell. Biol.* 18, 3112-3119.

Wang, K.H., Majewska, A., Schummers, J., Farley, B., Hu, C., Sur, M., Tonegawa, S., 2006. *In vivo* two-photon imaging reveals a role of arc in enhancing orientation specificity in visual cortex. *Cell* 126, 389-402.

Wilson, Y., Nag, N., Davern, P., Oldfield, B.J., McKinley, M.J., Greferath, U., Murphy, M., 2002. Visualization of functionally activated circuitry in the brain. *Proc. Natl. Acad. Sci. U.S.A.* 99, 3252-3257.

Wirtshafter, D., Asin, K.E., Pitzer, M.R., 1994. Dopamine agonists and stress produce different patterns of Fos-like immunoreactivity in the lateral habenula. *Brain Res.* 633, 21-26.

Worley, P.F., Bhat, R.V., Baraban, J.M., Erickson, C.A., McNaughton, B.L., Barnes, C.A., 1993. Thresholds for synaptic activation of transcription factors in hippocampus: correlation with long-term enhancement. *J. Neurosci.* 13, 4776-4786.

Yamaguchi, T., Danjo, T., Pastan, I., Hikida, T., Nakanishi, S., 2013. Distinct roles of segregated transmission of the septo-habenular pathway in anxiety and fear. *Neuron* 78, 537-544.

Zangenehpour, S., Chaudhuri, A., 2002. Differential induction and decay curves of c-fos and zif268 revealed through dual activity maps. *Brain Res. Mol. Brain Res.* 109, 221-225.

Figure legends

Figure 1.

Unilateral Venus labeling in the FR during postnatal development. In the coronal section, the left FR is labeled at P13 (*arrow head*) (**a**). The sheath of the FR is segmentally labeled (coronal: **b, c**; parasagittal: **d**). The cytoarchitecture is shown with the fluorescent Nissl stain (purple in **b–d**). The FR is rarely labeled before P10, unilaterally labeled between P11 and P20. The labeling is observed mainly in the right side in P11 and P12, whereas it was observed in both sides in P13 to P20. The FR is not labeled after P35 (**e**). Percentages of the labeled side are shown (**f**). Percentages of the labeled side in male and female mice are shown (**g**). *LHb*, lateral habenular nucleus; *FR*, fasciculus retroflexus; *R*, right; *L*, left. Scale bars, 300 μm (**a, d**) and 100 μm (**b, c**). In **e–g**, light gray and dark gray bars indicate the right (*R*) and left (*L*) sides of the labeled FR, respectively. White bars indicate that neither side of the FR was labeled (*No label*). *n* indicates the number of mice tested.

Figure 2.

ZIF268/EGR1-immunopositive cells in the LHb at P12. The coronal sections are from the mouse indicated with # in Fig. 3. The immunopositive cells are evenly distributed in the anterior LHb (**a, b**). They form medial clusters (*open arrowheads*) and lateral clusters (*closed arrowheads*) in the posterior LHb (**c, d**). *MHb*, medial habenular nucleus; *LHb*, lateral habenular nucleus. Right and left sides of the anterior LHb (**a** and **b**, respectively). Right and left sides of the posterior LHb (**c** and **d**, respectively). Scale bar, 100 μm .

Figure 3.

Transient lateralized activation in the LHb during postnatal development. Average number of ZIF268/EGR1-immunopositive cells in both sides, *R* + *L*, are shown (**a**). The number of

immunopositive cells is increased from P11 to P16. *** and ** indicate significant differences ($p < 0.001$ and $p < 0.01$, respectively, Kruskal-Wallis rank sum tests and Bonferroni multiple comparisons test). Average differences in the number of immunopositive cells between the right and left sides, $R - L$, are shown **(b)**. The differences are not significantly different from zero with Wilcoxon signed-rank tests. Average absolute values of the differences between the right and left sides, $|R - L|$, are shown **(c)**. ** and * indicate significant differences from zero ($p < 0.01$ and $p < 0.05$, respectively, Wilcoxon signed-rank tests). The number of ZIF268/EGR1-immunopositive cells in the anterior **(d)** and posterior LHb **(e)** in each mouse at P12. Light gray and dark gray bars indicate the numbers of positive cells in the right and left sides (R and L , respectively). Each mouse is indicated by roman numerals ($i-vii$). Histology of the mouse indicated with # is shown in Fig. 2.

Figure 4.

Effects of water-immersion restraint stress on FR labeling. The experimental design; fixation before the stress (*Ctrl*) and immediately (0), 1 (1), 3 (3), 6 (6), 12 (12), or 24 h (24) after the stress **(a)**. FR labeling is induced in either side **(b)**. The labeling is observed in the core and sheath of the FR **(c)**. Time course of the labeling after the stress is shown **(d)**. The labeling is observed in the right side at 6hr after the stress, whereas the labeling was observed in both sides at 24 hr after the stress. During postnatal development, the labeling is induced on P10, but not on P35 or later **(e)**. Light gray and dark gray bars indicate the labeling of the right (R) and left (L) sides of the FR, respectively. White bars indicate that neither side of the FR was labeled (*No label*). *FR*, fasciculus retroflexus. R , right. L , left. Scale bars, 100 μm .

Figure 5.

Lateralized activation in the LHb induced by water-immersion restraint stress. Average

number of ZIF268/EGR1-immunopositive cells in both sides, R + L, are shown **(a)**. * indicates a significant difference ($p < 0.05$, Kruskal-Wallis rank sum test and Bonferroni multiple comparisons test). Average differences of the immunopositive cells in the right and left sides, R – L, are shown **(b)**. The differences are not significantly different from zero with Wilcoxon signed-rank tests. Average absolute values of the differences, |R – L|, are shown **(c)**. ** and * indicate significant differences from zero ($p < 0.01$ and $p < 0.05$, respectively, Wilcoxon signed-rank tests). Neuronal activities in the PV and DG are shown **(d-i)**. Average number of ZIF268/EGR1-immunopositive cells in both sides of the PV, R + L, are shown **(d)**. ** indicates a significant difference ($p < 0.01$, Kruskal-Wallis rank sum test and Bonferroni multiple comparisons test). Average differences in the number of immunopositive cells in the right and left sides of the PV, R – L, are shown **(e)**. * indicates a significant difference from zero ($p < 0.05$, Wilcoxon signed-rank tests). Average absolute values of the differences in the right and left PV, |R – L|, are shown **(f)**. ** and * indicate significant differences from zero ($p < 0.01$ and $p < 0.05$, respectively, Wilcoxon signed-rank tests). Average number of immunopositive cells in both sides of the DG, R + L, are shown **(g)**. They are not significantly different with Kruskal-Wallis rank sum tests. Average differences in the number of immunopositive cells in the right and left sides of the DG, R – L, are shown **(h)**. They are not significantly different from zero with Wilcoxon signed-rank tests. Average absolute values of the differences in the right and left DG, |R – L|, are shown **(i)**. ** and * indicate significant differences from zero ($p < 0.01$ and $p < 0.05$, respectively, Wilcoxon signed-rank tests). Hours after water-immersion restraint stress are indicated.

Figure 6.

Topographic activation of the LHb along the anterior-posterior axis induced by water-immersion restraint stress. Distribution of ZIF268/EGR1-immunopositive cells are

shown in the anterior (**a**) and posterior (**b**) LHb 1h after the stress, and in the anterior (**c**) and posterior (**d**) LHb 3 h after the stress. Squares indicate autofluorescence of the fasciculus retroflexus (**b** and **d**). Average number of ZIF268/EGR1-immunopositive cells in both sides of the LHb, R + L, are shown (**e**). * indicates a significant difference ($p < 0.05$, Kruskal-Wallis rank sum tests and Bonferroni multiple comparisons test). Average differences of the immunopositive cells between the right and left sides, R – L, are shown (**f**). The differences are not significantly different from zero with Wilcoxon signed-rank tests. Average absolute values of the differences between the right and left LHb, |R – L|, are shown (**g**). ** and * indicate significant differences from zero ($p < 0.05$ and $p < 0.01$, respectively, Wilcoxon signed-rank tests). Hours after water-immersion restraint stress are indicated. Dark gray and light gray bars indicate the *anterior LHb* and *posterior LHb*, respectively. Scale bar, 100 μm .

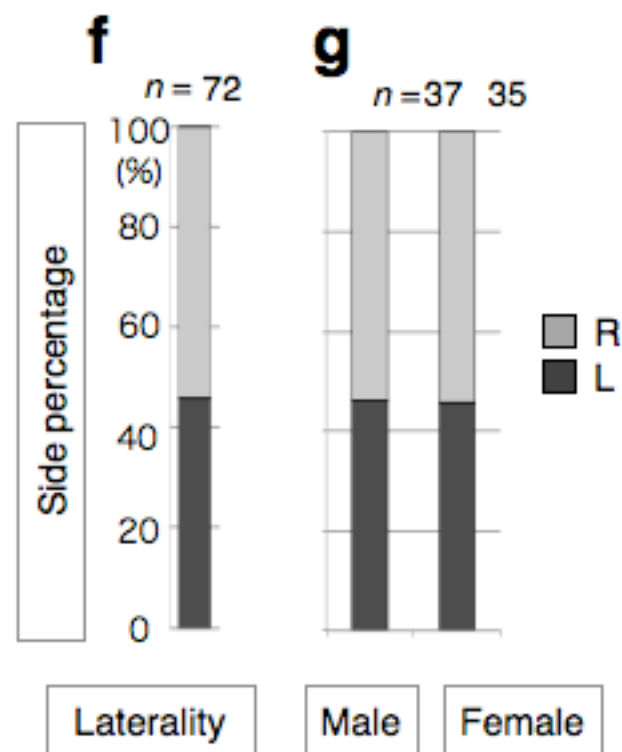
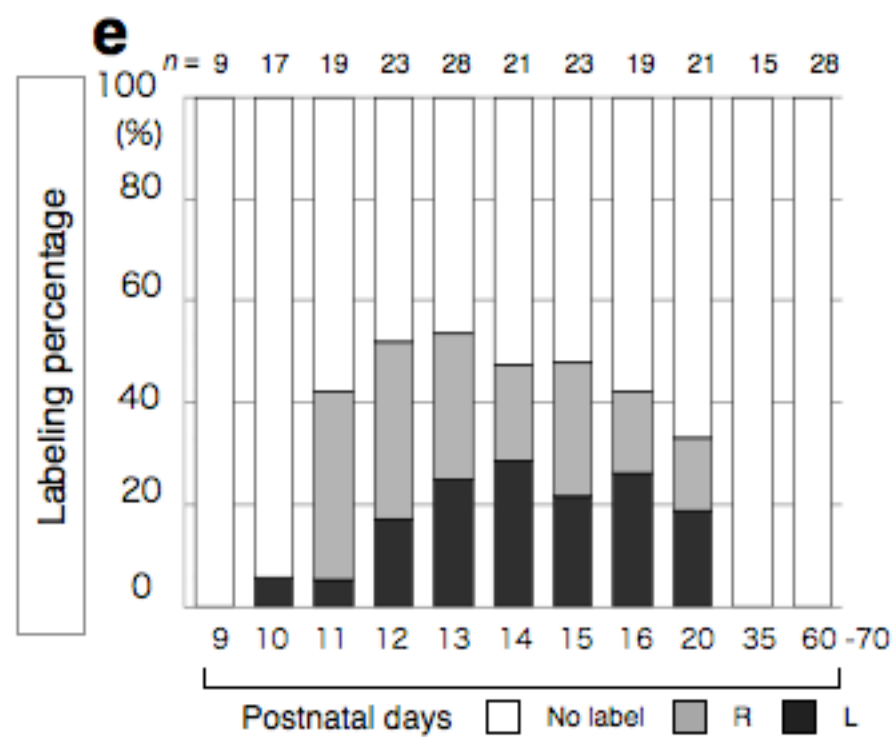
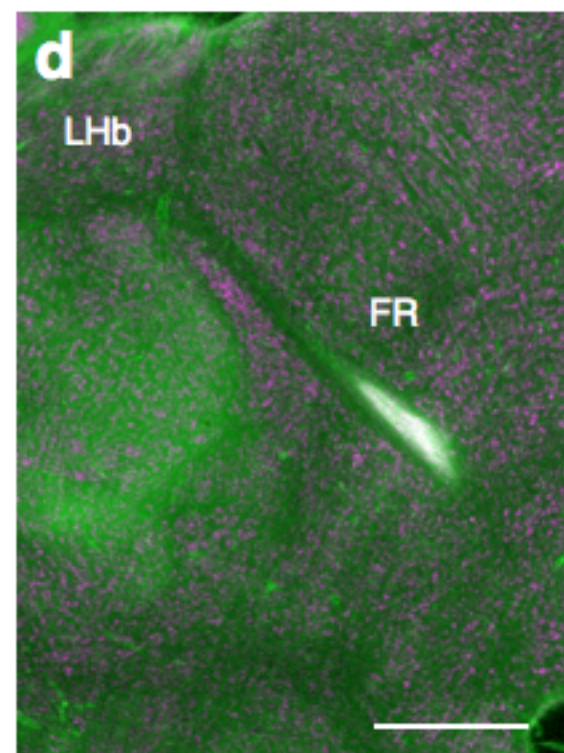
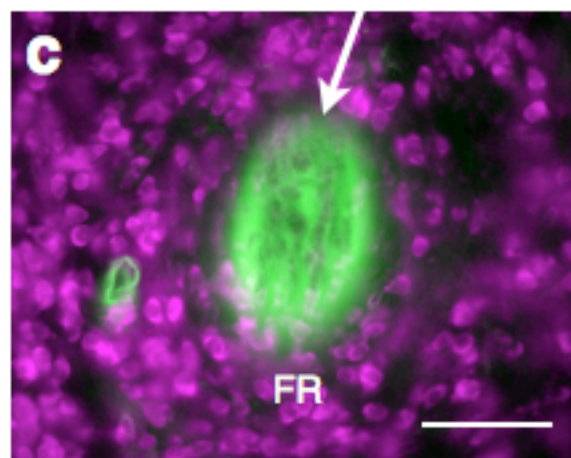
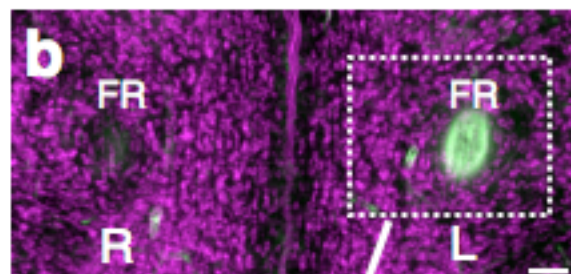
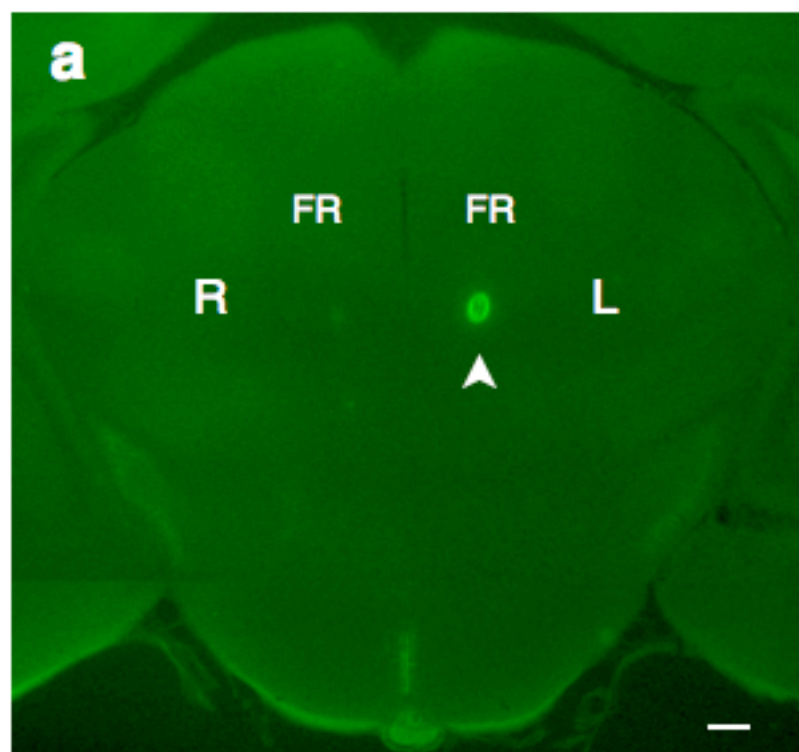


Figure 1

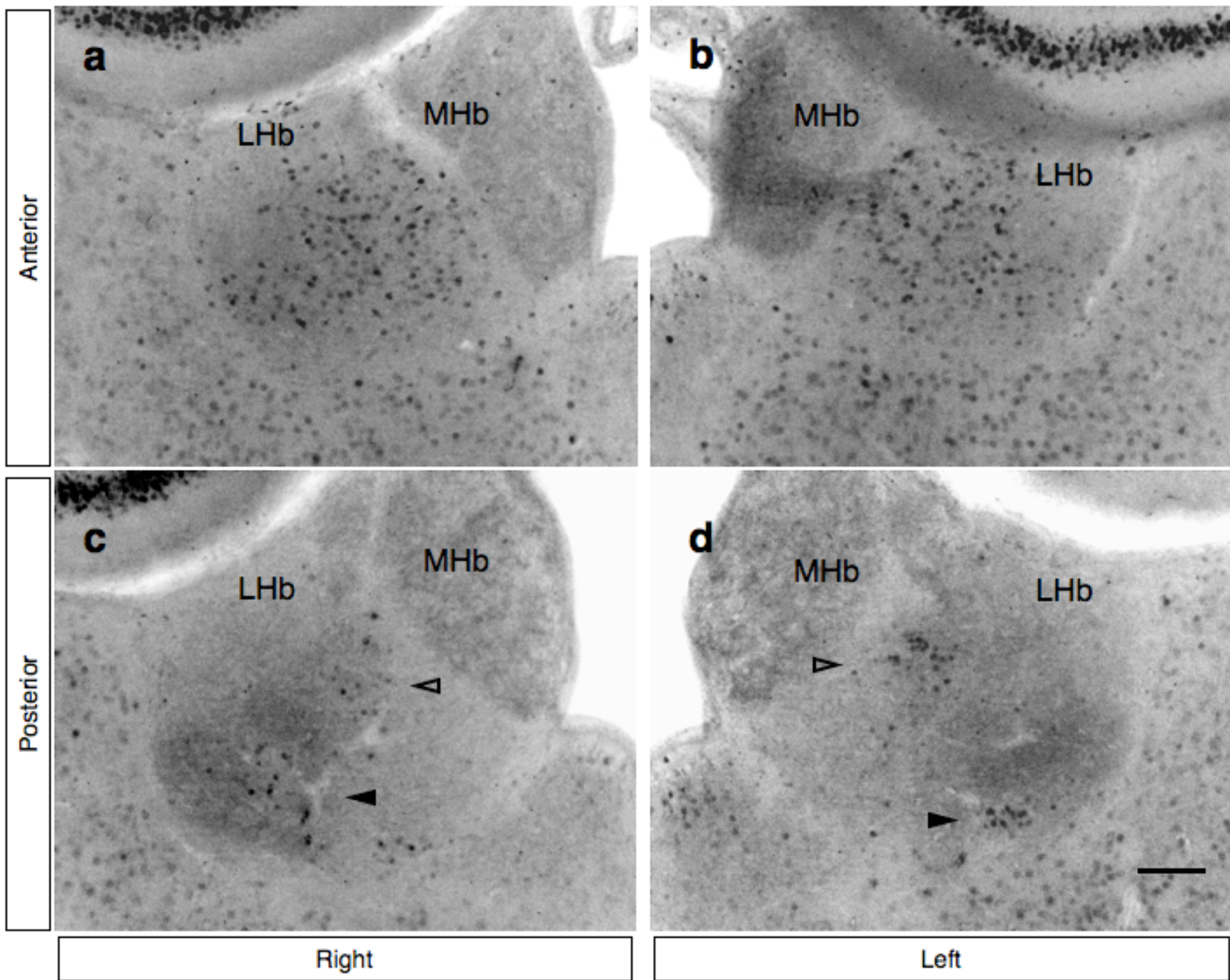


Figure 2

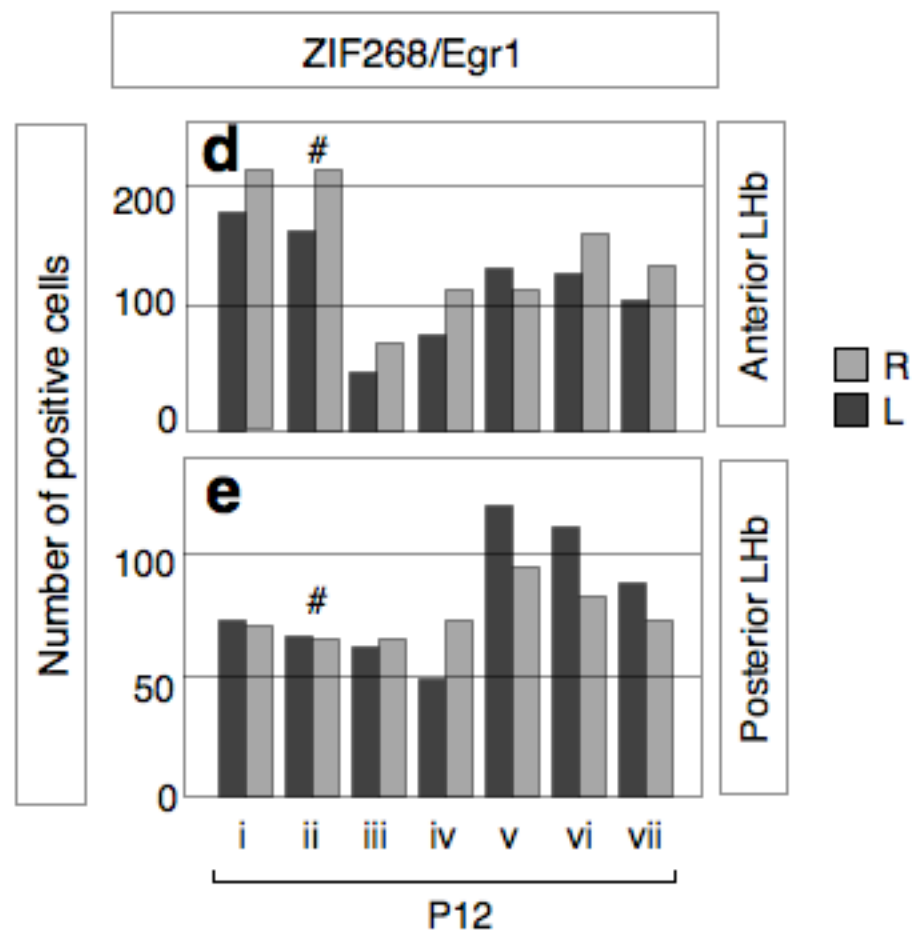
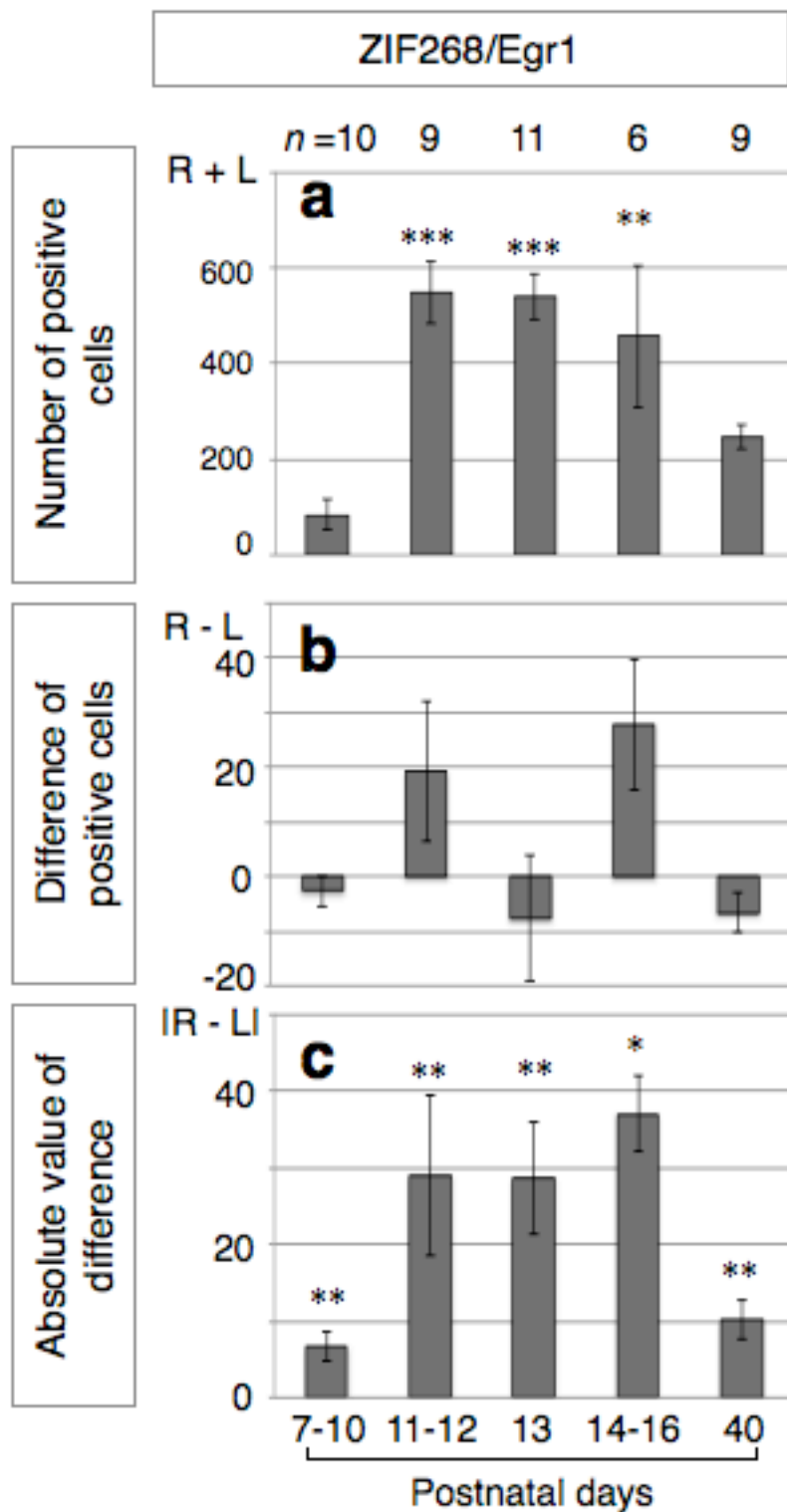


Figure 3

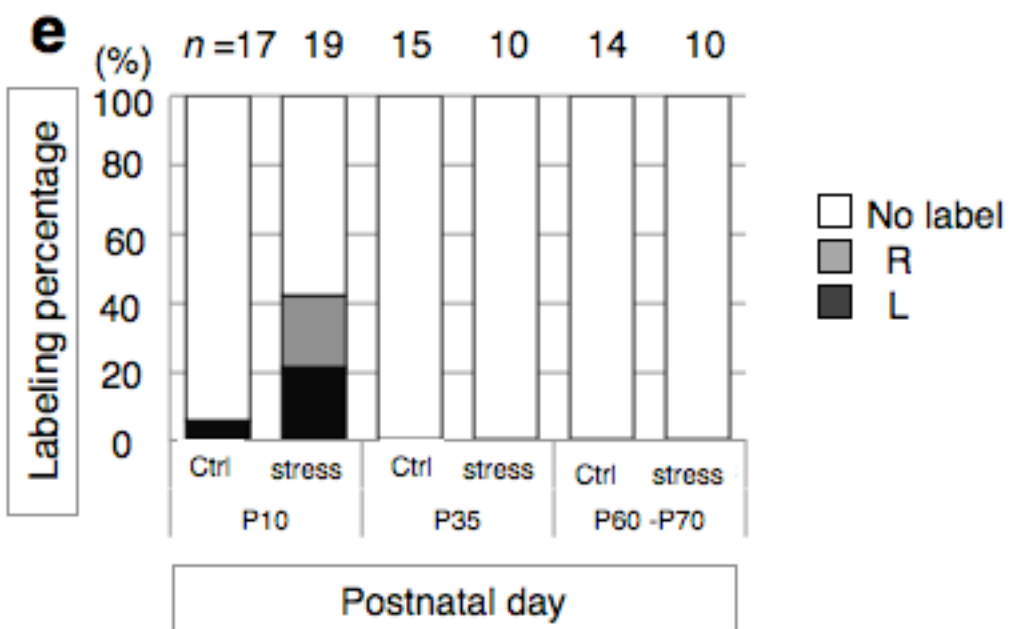
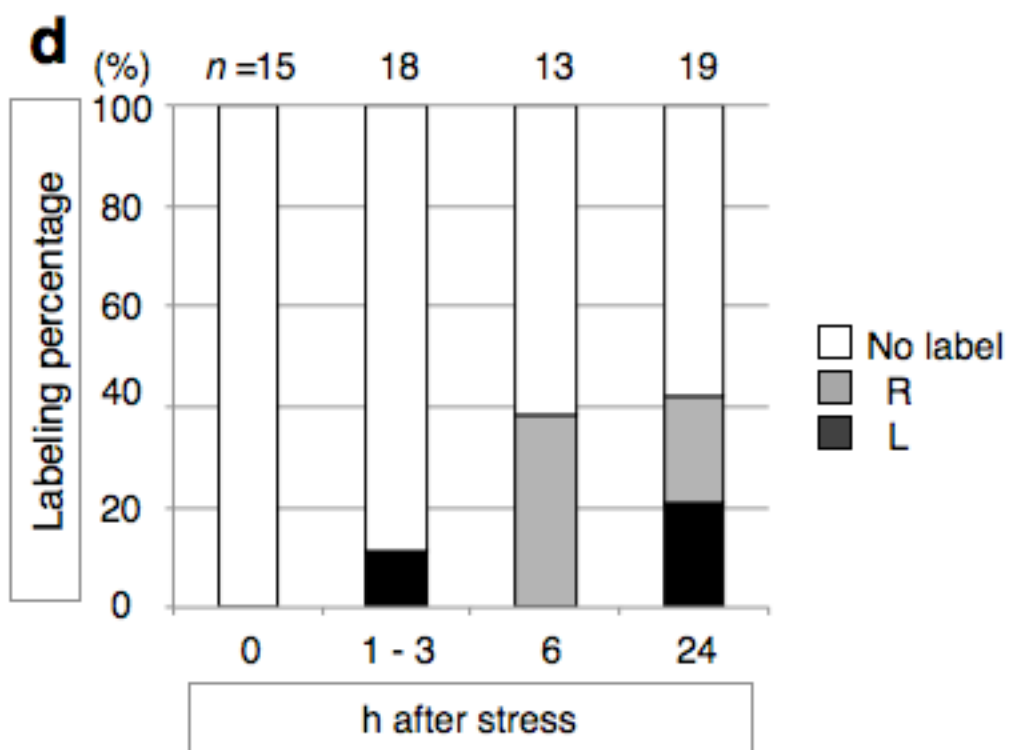
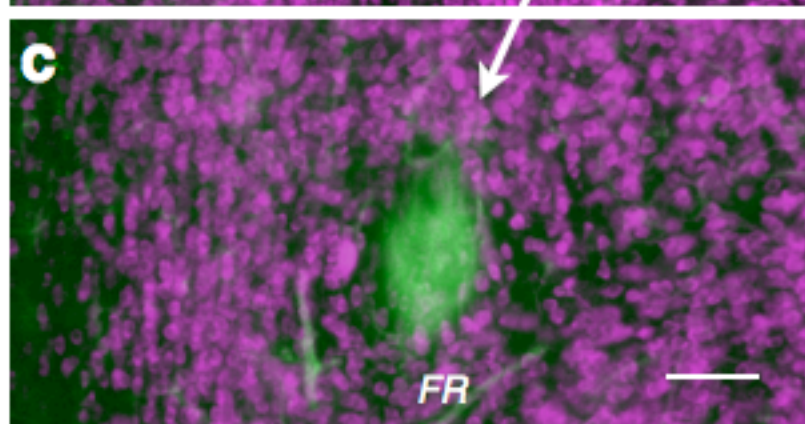
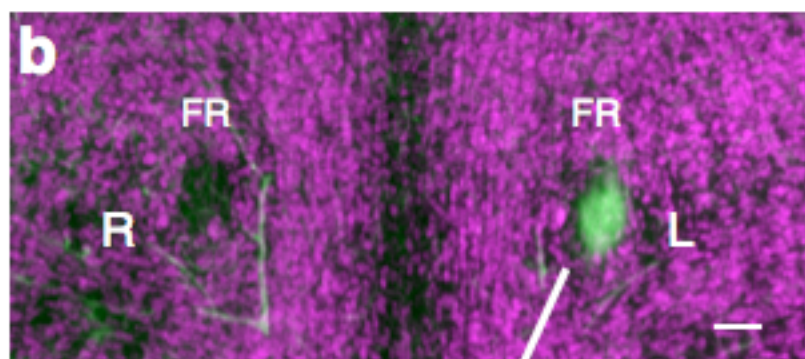
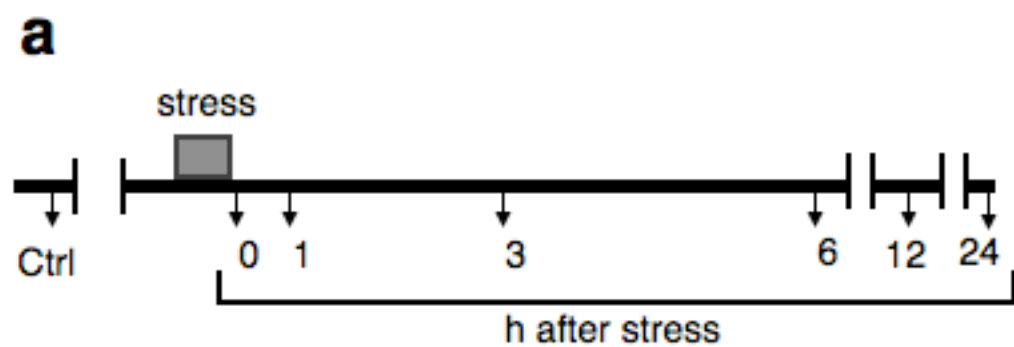


Figure 4

Number of positive cells

Difference of positive cells

Absolute value of difference

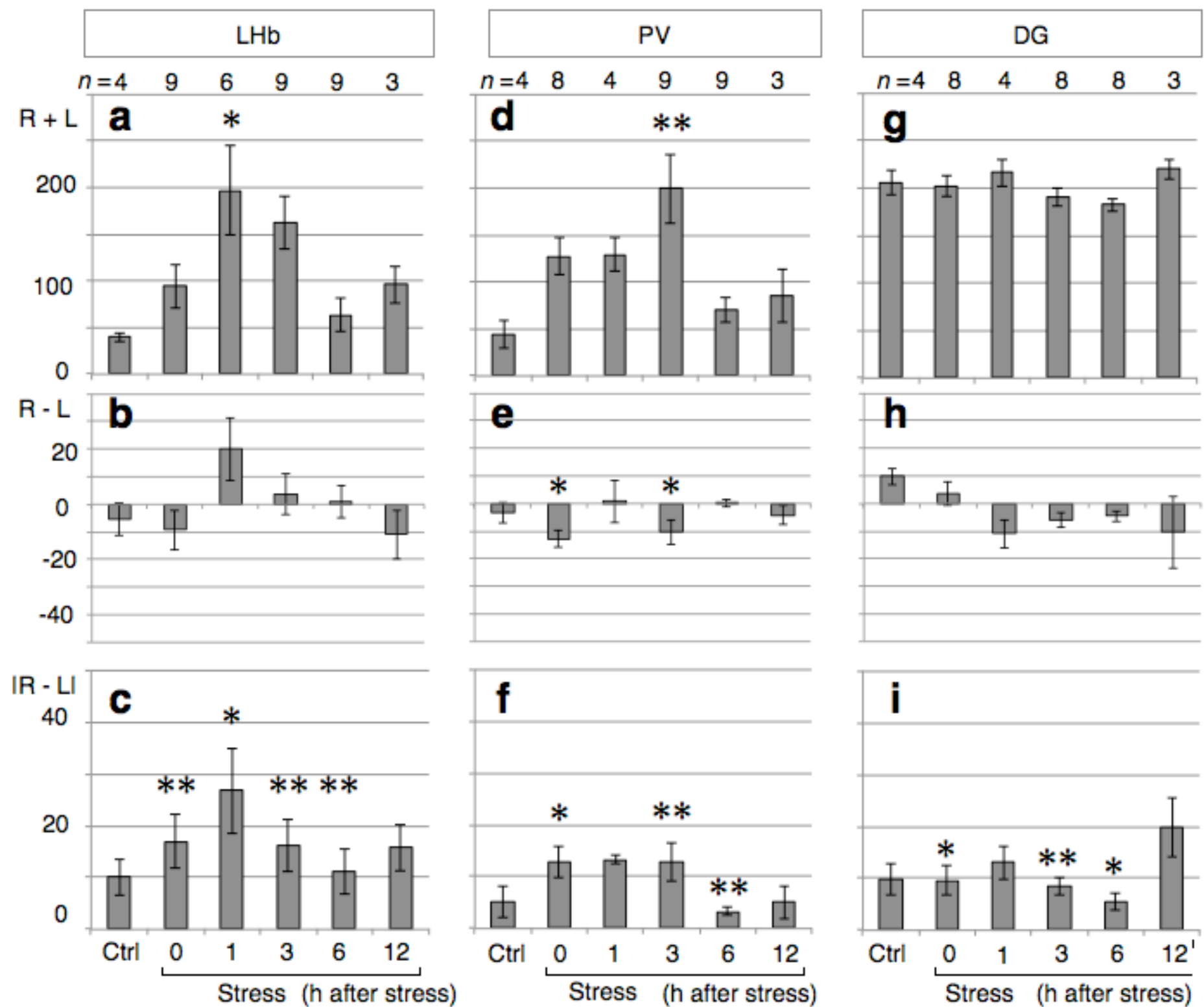


Figure 5

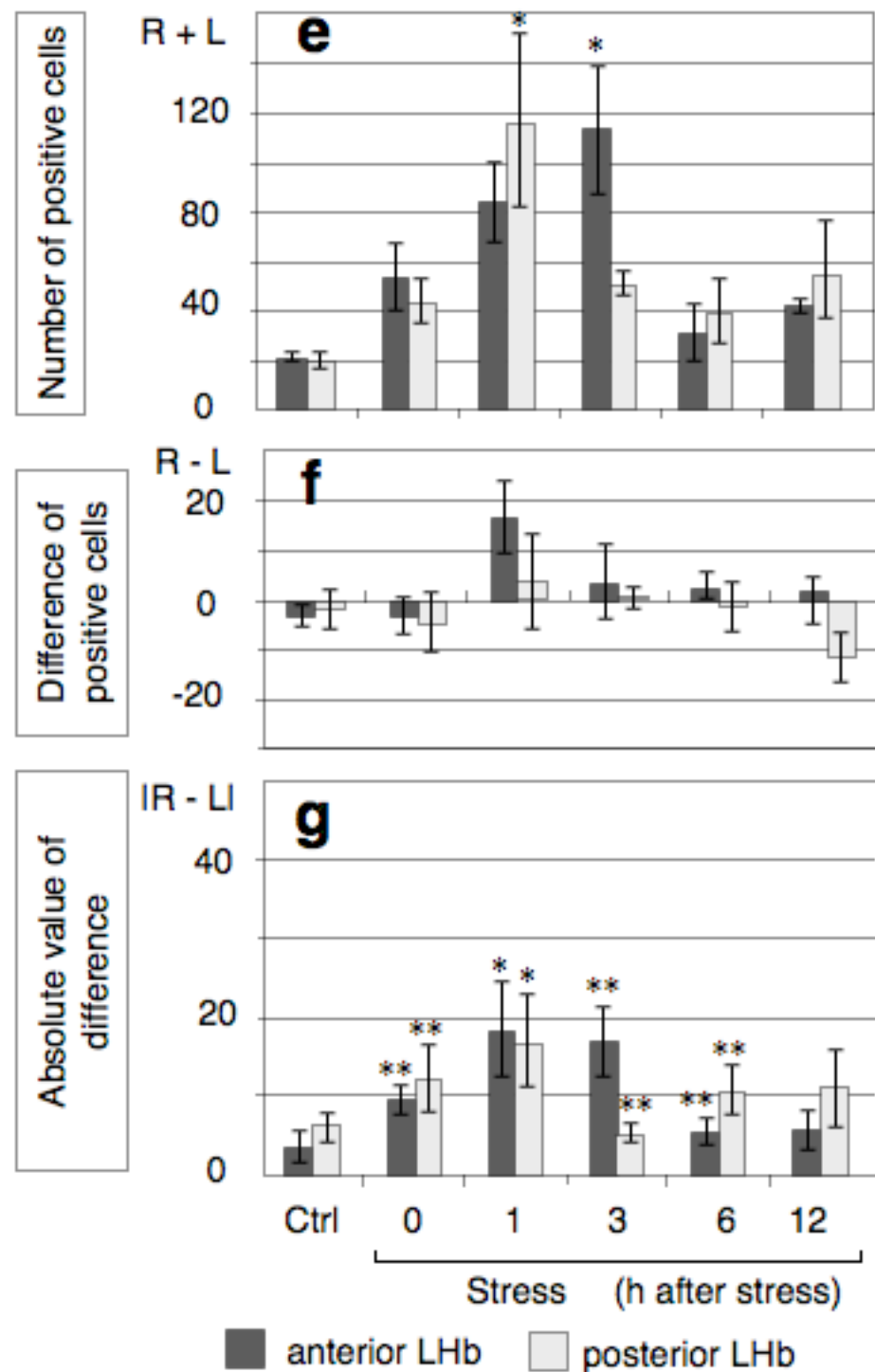
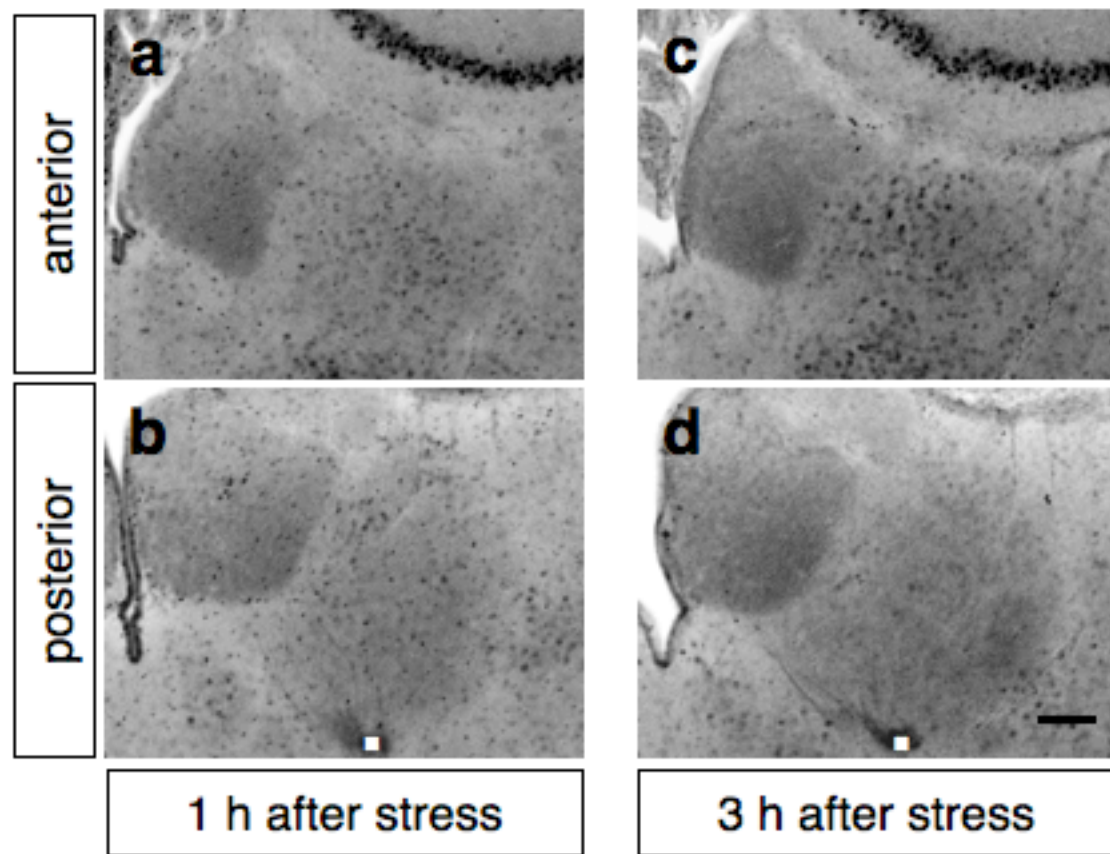


Figure 6